

Pairing Effects at the Fission Saddle Point of ^{210}Po and $^{211}\text{Po}^\dagger$

L. G. MORETTO,* R. C. GATTI, AND S. G. THOMPSON

Lawrence Radiation Laboratory, University of California, Berkeley, California 94720

AND

J. R. HUIZENGA

Department of Chemistry and Physics, University of Rochester, Rochester, New York 14627

AND

J. O. RASMUSSEN

Departments of Chemistry and Physics, University of California, Berkeley, California 94720

(Received 9 September 1968)

The fission-fragment angular distributions were measured for ^4He -induced fission of ^{206}Pb and ^{207}Pb targets. The compound nuclei ^{210}Po and ^{211}Po were obtained at excitation energies ranging from 3 to 20 MeV above the fission barriers. The experimental data were fitted by a theoretical expression relating the angular distribution of fission fragments to the distribution of the total angular momentum I and of the angular momentum projection K on the nuclear symmetry axis at the saddle point. By a least-squares fitting procedure, the variance K_0^2 of the K distribution was obtained. In the case of the even-even nucleus ^{210}Po , the K_0^2 value approaches zero at about 3 MeV above the barrier, while in the case of the odd- A nucleus ^{211}Po , K_0^2 remains rather large. This indicates the presence of the pairing gap in ^{210}Po and of the residual quasiparticle in ^{211}Po . Furthermore, the approximately constant difference in K_0^2 between the even-even and odd- A nucleus at corresponding energies is consistent with the expected contribution of a single quasiparticle to K_0^2 . From the analysis of the data, the value of the pairing gap 2Δ at the saddle point of ^{210}Po is estimated to be about 4 MeV, about two to three times larger than in the ground state. The odd-even differences of saddle-point masses are also analyzed and the dependence of pairing on the nuclear surface is discussed.

I. INTRODUCTION

NUCLEI in their fission saddle-point configurations exhibit "transition state" spectra which resemble those of deformed nuclei in their stable equilibrium configurations.¹ In general, however, the fission saddle point is characterized by much larger deformations than those of the ground-state nuclei. Therefore, the study of nuclei at the saddle point can provide information about nuclear properties at unusually large deformations. The properties of the transition-state nuclei can be investigated by measurements of fission-fragment angular distributions.

While at very small excitation energies above the barrier the angular distributions can be interpreted in terms of a few transition-state levels, at energies larger than a few MeV only a statistical analysis is possible. Halpern and Strutinski² and Griffin³ have used the assumption of statistical distribution of levels at the saddle point to calculate the angular distributions at medium-low excitation energies and attempted to fit experimental data. The energy dependence was deter-

mined in terms of the Fermi gas model. The conclusion of the analysis seems to be that, while the shape of the angular distributions is reproduced very well, the expected dependence on the excitation energy is verified by the experiment no more than qualitatively. The idea that at relatively low excitation energies the Fermi gas model is expected to fail and that the pairing effects must be considered has been expressed by Halpern and Strutinski,² Griffin,⁴ and Vandenbosch *et al.*⁵

An attempt to measure the saddle-point pairing effects was made by Griffin,⁶ who analyzed angular distribution data of Vandenbosch *et al.*⁵ on ^{237}Pu and of Simmons⁷ on ^{240}Pu compound nuclei. The gap parameter obtained was $\Delta_0 = 1.36$ MeV, which implied a pairing gap of $2\Delta_0 = 2.72$ MeV for ^{240}Pu . This value is more than twice the value in the ground state. Further experiments by Britt *et al.*^{8,9} using $^{239}\text{Pu}(d, pf)$ reaction succeeded in estimating the value $2\Delta_0 = 2.6(+0.21, -0.45)$ MeV for ^{240}Pu at the saddle point. More recent experiments by

[†] Work performed under the auspices of the U.S. Atomic Energy Commission.

* On leave from University of Pavia, Pavia, Italy.

¹ A. Bohr, in *Proceedings of the First United Nations International Conference on the Peaceful Uses of Atomic Energy* (United Nations, New York, 1956), Vol. 2, p. 151, Paper P/911.

² I. Halpern and V. M. Strutinski, in *Proceedings of the Second United Nations International Conference on the Peaceful Uses of Atomic Energy* (United Nations, Geneva, 1958), Vol. 15, p. 408, Paper P/1513.

³ J. J. Griffin, *Phys. Rev.* **116**, 107 (1959).

⁴ J. J. Griffin, in *Proceedings of the International Conference on Nuclear Structure, Kingston, Canada, 1960*, edited by D. A. Bromley and E. W. Vogt (University of Toronto Press, Toronto, Canada, 1960), p. 843.

⁵ R. Vandenbosch, H. Warhanek, and J. R. Huizenga, *Phys. Rev.* **124**, 846 (1961).

⁶ J. J. Griffin, *Phys. Rev.* **132**, 2204 (1963).

⁷ J. E. Simmons, R. B. Perkins, and R. L. Henkel, *Phys. Rev.* **137**, B809 (1966).

⁸ H. Britt, R. Stokes, W. Gibbs, and J. J. Griffin, *Phys. Rev. Letters* **11**, 343 (1963).

⁹ H. Britt, R. Stokes, W. Gibbs, and J. J. Griffin, *Phys. Rev.* **139**, B345 (1965).

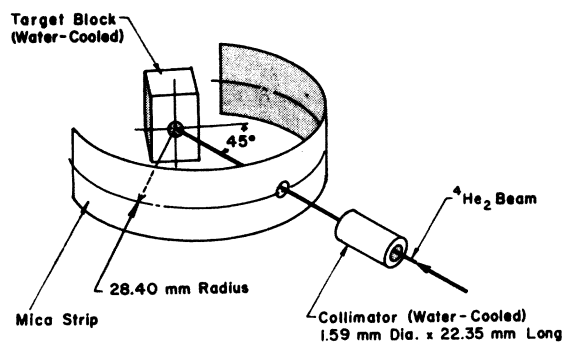


FIG. 1. Schematic drawing of the apparatus used in measuring angular distributions of fission fragments.

Rickey and Britt¹⁰ gave the value $2\Delta_0 = 1.98 \pm 0.15$ MeV for ^{240}Pu and $2\Delta_0 = 2.10 \pm 0.15$ MeV for ^{238}U .

The rather large value of the pairing effects at the saddle point was observed much earlier by Swiatecki¹¹ in his investigation of the even-odd mass differences at the saddle point of nuclei heavier than thorium. He observed that while the odd-odd, odd, and even-even families of nuclear masses in the ground state are separated by about 0.77 mmu, at the saddle point the same families are separated by about 1.2 mmu. Fong¹² also discusses the same effect. This increase in pairing effects in the transition-state spectrum was attributed¹³ to the increase in surface area of the nucleus at the saddle point. Some calculations by Kennedy *et al.*¹³ on the slab model of a nucleus show that while infinite

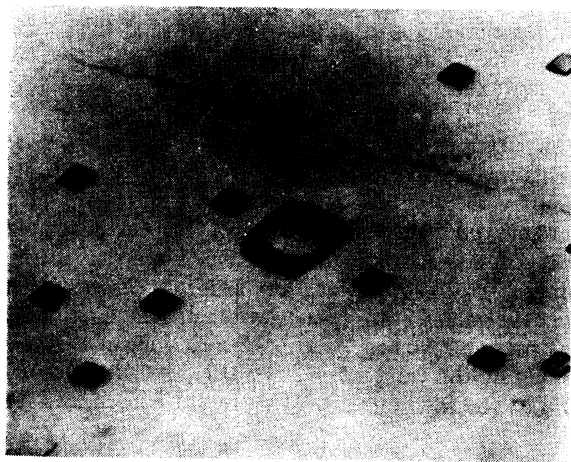


FIG. 2. Fission tracks in mica. Etching: 6 h at room temperature in 48% hydrofluoric acid. The fission fragments have entered perpendicularly to the mica surface; therefore the picture shows the normal sections of the tracks. The large track is a pre-etched background track due to spontaneous fission of U^{238} in mica.

¹⁰ F. A. Rickey, Jr., and H. C. Britt, *Bull. Am. Phys. Soc.* **13**, 36 (1968).

¹¹ W. Swiatecki, *Phys. Rev.* **100**, 936 (1955).

¹² P. Fong, *Phys. Rev.* **122**, 1545 (1961).

¹³ R. C. Kennedy, L. Wilets, and E. M. Henley, *Phys. Rev. Letters* **12**, 36 (1964).

nuclear matter presented vanishingly small pairing effects, the slab-model calculations predicted a finite pairing gap very sensitive to the slab thickness.

To shed more light on the problem we attempted to determine the pairing effects at the saddle points of ^{210}Po and ^{211}Po . The reason for this choice is twofold: (a) The increase in surface area at the saddle point is for these nuclei $\sim 20\%$ according to liquid-drop calculations,¹⁴ while for ^{240}Pu it is 10% relative to the spherical shape and less when one considers the deformation already present in the ground state. (b) The fission probability near the barrier, though very low, is still sufficient to allow the measurement of fission-fragment

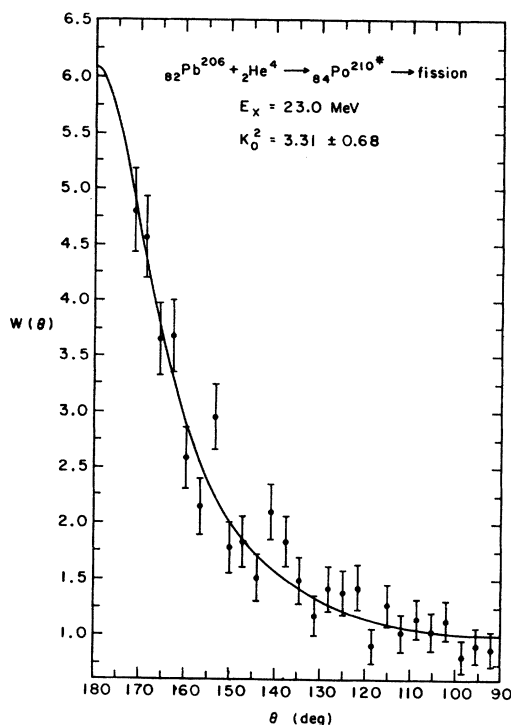


FIG. 3. Center-of-mass angular distribution of fission fragments in 29-MeV- He^4 -induced fission of Pb^{206} . The continuous line is the least-squares fit to the experimental data.

angular distributions. The reason for the choice of the even-odd pair was the expectation that systematic even-odd differences in the properties of the transition spectrum could be observed.

II. THEORETICAL EXPRESSION FOR THE ANGULAR DISTRIBUTION

An axially symmetric nucleus at the fission saddle point is characterized by three angular momentum quantum numbers which are the total angular momentum I , the projection of I on the space-fixed z axis M ,

¹⁴ James Rayford Nix, University of California Radiation Laboratory Report No. UCRL-17958, 1968 (unpublished).

and the projection of I on the body-fixed symmetry axis K . If K stays constant from the saddle point to infinity, the probability distribution of the symmetrical top wave function at the saddle point determines the fission-fragment angular distribution. The constancy of K is classically dependent on the preservation of axial symmetry from saddle to infinity; this assumption is partially supported by the liquid-drop model which predicts axially symmetric saddle-point shapes, and by the pairing effects which tend to preserve axial symmetry. Furthermore, the stage between saddle and scission point seems to be so short¹⁴ that the Coriolis interaction might be prevented from effectively mixing levels with different K . If some limited K mixing from Coriolis or γ -vibrational interactions is present, the theoretical approach may still be valid. A strong evidence of the goodness of the K quantum number from the saddle point to infinity comes from the sharpness of the experimental angular distributions themselves. Assuming then that K is a good quantum number, the angular distribution of fission fragments from a system characterized by a given set of I , M , K values will be

$$W_{M,K^I}(\theta) = [(2I+1)/4\pi] |D_{M,K^I}(\phi, \theta, \chi)|^2, \quad (1)$$

where D_{M,K^I} is the symmetrical-top wave function and ϕ , θ , and χ are the Eulerian angles that define the position of the body with respect to the rest frame of reference.

Since the quantity D_{M,K^I} can be written explicitly as

$$D_{M,K^I}(\phi, \theta, \chi) = d(\theta) e^{iM\phi} e^{iK\chi}, \quad (2)$$

it follows that $|D_{M,K^I}|^2$ is a function only of the angle θ between the space-fixed and body-fixed axis.

$$W_{K_0^{2I}}(\theta) = \frac{2I+1}{4\pi^2} \left[\int_0^{(I+1/2)\sin\theta} dK [(I+\frac{1}{2})^2 \sin^2\theta - K^2]^{-1/2} \exp\left(\frac{-K^2}{2K_0^2}\right) / \int_0^{I+1/2} dK \exp\left(\frac{-K^2}{2K_0^2}\right) \right]. \quad (4)$$

The upper limit of the integral in the numerator represents the highest value of K which is classically possible at every angle θ . By executing the integration we have

$$W_{K_0^{2I}}(\theta) = \left(\frac{2}{\pi}\right)^{1/2} (4\pi)^{-1} \frac{(2I+1)}{2(K_0^2)^{1/2}} \left[\text{erf} \frac{I+\frac{1}{2}}{2(K_0^2)^{1/2}} \right]^{-1} \times \exp\left(-\frac{(I+\frac{1}{2})^2 \sin^2\theta}{4K_0^2}\right) J_0\left(i \frac{(I+\frac{1}{2})^2 \sin^2\theta}{4K_0^2}\right), \quad (5)$$

where erf is the error function and J_0 is the Bessel function of order zero.

The angular momentum distribution for the compound nucleus can be obtained by analyzing the reaction mechanism involved in its formation. In the present case, involving a particle bombardment with

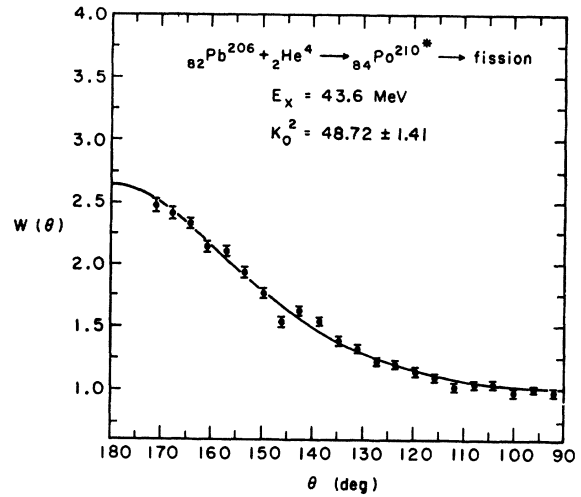


FIG. 4. Center-of-mass angular distribution of fission fragments in 50-MeV-He⁴-induced fission of Pb²⁰⁶. The continuous line is the least-squares fit to the experimental data.

For large I the angular distribution can be expressed in the following approximate form^{15,3}:

$$W_{M,K^I}(\theta) = [(2I+1)/4\pi^2] \times [(I+\frac{1}{2})^2 \sin^2\theta - M^2 - K^2 + 2MK \cos\theta]^{-1/2}. \quad (3)$$

In order to reproduce the angular distributions of fission fragments obtained in particle bombardments, the above expression must be averaged over the K and I distributions.

Following Halpern and Strutinski,² we assume the K distribution to be of the form $\exp(-K^2/2K_0^2)$. If $M=0$, for fixed I and K_0^2 the angular distribution will be

compound nucleus formation, the total angular momentum distribution can be obtained from an optical-model calculation.

If we assume that the nuclei at the saddle point have the same I distribution as the compound nucleus, the final angular distribution averaged over K and I will then be

$$W(\theta) \propto \sum_{I=0}^{\infty} (2I+1)^2 T_I \left[\text{erf} \frac{I+\frac{1}{2}}{2(K_0^2)^{1/2}} \right]^{-1} \times \exp\left(-\frac{(I+\frac{1}{2})^2 \sin^2\theta}{4K_0^2}\right) J_0\left(i \frac{(I+\frac{1}{2})^2 \sin^2\theta}{4K_0^2}\right), \quad (6)$$

¹⁵ T. A. Wheeler, in *Fast Neutron Physics*, edited by J. B. Marion and J. L. Fowler (Wiley-Interscience Publishers, Inc., New York, 1963), Part II.

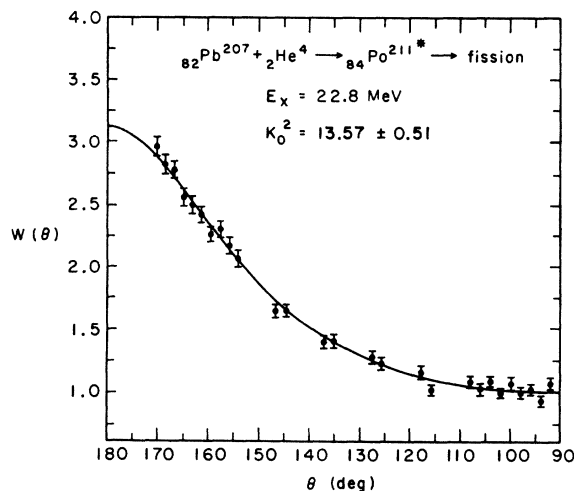


FIG. 5. Center-of-mass angular distribution of fission fragments in 31-MeV- He^4 -induced fission of Pb^{207} . The continuous line is the least-squares fit to the experimental data.

where T_I are the optical-model transmission coefficients. This approximate expression has been shown to be very satisfactory when compared with the expression obtained using the symmetrical-top wave functions in their exact quantum-mechanical form.¹⁶

III. EXPERIMENTAL PROCEDURE

The experiments were designed to measure the fission-fragment angular distributions of He^4 -induced fission of Pb^{206} and Pb^{207} . The lowest excitation energy for which angular distributions were measured was about 3 MeV above the fission barrier. The highest excitation energy, about 20 MeV above the barrier, was determined on the basis of substantial onset of multiple-chance fission as estimated from the cross-section data.

Mica was used for detecting the fission fragments¹⁷ because of its good performance and convenience when very small cross sections are involved, as was the case here. The experimental setup consisted of a small fission chamber as indicated in Fig. 1, in which a mica holder was fitted. The mica strip was laid on a cylindrical surface whose radius was 2.84 cm. The exposed surface of mica ranged in angle from 45° to 205° with respect to the beam direction. At 205° a shield was used to cover the mica and give a sharp cutoff in the fission-fragment distribution, which served as an angular reference point. The height of the exposed part of the mica strip was 1 cm.

Particular care was taken in preparing high-purity targets because of the very low cross sections

($<10^{-32}$ cm^2) at the lowest excitation energies above the barrier. With such cross sections even one part in 10^9 of uranium or thorium would contribute enough fission events to cause a substantial error in the experiment. The target backing consisted of a water-cooled copper block that was fitted in the center of the chamber at an angle of 45° with respect to the beam direction. The surface on which the target material was to be deposited was first covered with a thickness of more than 20 mg/cm^2 of high-purity silver deposited by evaporation. This layer prevented fission fragments coming from the impurities in the copper from escaping and entering the mica. The target materials, mono-isotopic ^{206}Pb and ^{207}Pb in the form of metal, were evaporated on the silver. In preparing the targets by vaporization of the lead isotopes, early and late fractions of the distillate were excluded since they are most likely to contain the highest levels of impurities. It is especially desirable to avoid collecting the late fractions because the uranium and thorium impurities tend to concentrate there. The purity of the targets was checked by two methods. The first involved bombarding at energies below the fission barriers of ^{210}Po and ^{211}Po and searching for fission events which might come from impurities with lower fission barriers, such as uranium or thorium. The second method consisted in checking the steepness of the cross-section curves as a function of energy at energies near the barrier.

The thickness of the targets ranged between 1 and 3 mg/cm^2 . The effects of the thickness of the target on the angular distributions were determined experimentally and found to be negligible up to 3 mg/cm^2 thickness for angles between 85° and 175° . The position of the beam on the target was determined by a collimator 22.35-mm long and 1.59 mm in diameter and by the

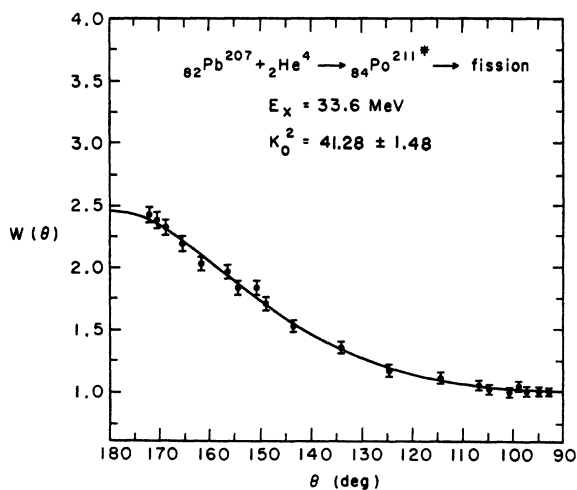


FIG. 6. Center-of-mass angular distribution of fission fragments in 42-MeV- He^4 -induced fission of Pb^{207} . The continuous line is the least-squares fit to the experimental data.

¹⁶ J. R. Huizenga, A. N. Behkami, and L. G. Moretto (unpublished).

¹⁷ P. B. Price and R. M. Walker, *J. Appl. Phys.* **33**, 2625 (1962); **33**, 3407 (1962).

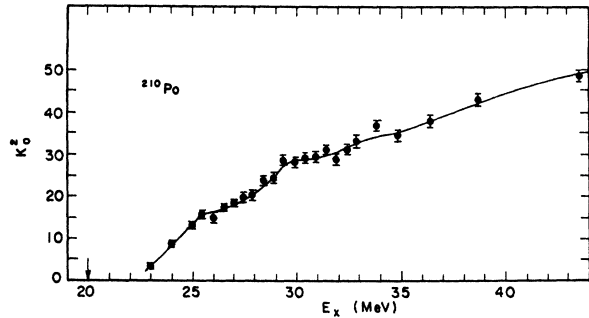


FIG. 7. K_0^2 dependence on excitation energy at the fission saddle point of Po^{210} . The arrow indicates the position of the fission barrier.

low convergence of the beam, controlled by a quadrupole focussing lens 7 m away from the collimator. The beam current was read from the target itself without a separate Faraday cup.

The variable energy beam of the ^4He particles was provided by the 88-in. variable-frequency cyclotron in

TABLE I. K_0^2 versus excitation energy in ^{210}Po fission.

| E_{lab} (MeV) | E_x (MeV) | K_0^2 | Anisotropy $W(180^\circ)/W(90^\circ)$ | $\langle l^2 \rangle$ |
|------------------------|-------------|------------------|---------------------------------------|-----------------------|
| 29.0 | 23.0 | 3.31 ± 0.68 | 6.05 ± 0.54 | 89.723 |
| 30.0 | 24.0 | 8.85 ± 0.58 | 3.73 ± 0.13 | 99.400 |
| 31.0 | 25.0 | 13.14 ± 0.63 | 3.16 ± 0.08 | 109.154 |
| 31.5 | 25.5 | 15.86 ± 0.66 | 2.92 ± 0.07 | 114.052 |
| 32.0 | 26.0 | 14.91 ± 1.29 | 3.09 ± 0.14 | 118.960 |
| 32.5 | 26.5 | 17.61 ± 0.56 | 2.88 ± 0.05 | 123.877 |
| 33.0 | 27.0 | 18.40 ± 0.71 | 2.87 ± 0.06 | 128.801 |
| 33.5 | 27.4 | 20.11 ± 0.79 | 2.79 ± 0.06 | 133.731 |
| 34.0 | 27.9 | 20.60 ± 0.64 | 2.81 ± 0.05 | 138.664 |
| 34.5 | 28.4 | 23.96 ± 0.72 | 2.63 ± 0.04 | 143.601 |
| 35.0 | 28.9 | 24.47 ± 1.27 | 2.65 ± 0.07 | 148.539 |
| 35.5 | 29.4 | 28.67 ± 1.00 | 2.48 ± 0.04 | 153.480 |
| 36.0 | 29.9 | 28.41 ± 1.24 | 2.53 ± 0.06 | 158.420 |
| 36.5 | 30.4 | 29.54 ± 0.72 | 2.52 ± 0.03 | 163.361 |
| 37.0 | 30.9 | 29.79 ± 1.30 | 2.55 ± 0.06 | 168.302 |
| 37.5 | 31.4 | 31.17 ± 0.60 | 2.52 ± 0.02 | 173.242 |
| 38.0 | 31.9 | 28.94 ± 1.46 | 2.67 ± 0.07 | 178.180 |
| 38.5 | 32.4 | 31.43 ± 0.63 | 2.59 ± 0.03 | 183.117 |
| 39.0 | 32.8 | 33.57 ± 1.26 | 2.53 ± 0.05 | 188.052 |
| 40.0 | 33.8 | 36.13 ± 1.75 | 2.50 ± 0.06 | 197.916 |
| 41.0 | 34.8 | 34.47 ± 0.81 | 2.63 ± 0.03 | 207.769 |
| 42.6 | 36.4 | 38.05 ± 1.48 | 2.59 ± 0.05 | 223.510 |
| 45.0 | 38.7 | 42.96 ± 1.47 | 2.56 ± 0.04 | 247.058 |
| 50.0 | 43.6 | 48.72 ± 1.41 | 2.63 ± 0.04 | 295.853 |

TABLE II. K_0^2 versus excitation energy in ^{211}Po fission.

| E_{lab} (MeV) | E_x (MeV) | K_0^2 | Anisotropy $W(180^\circ)/W(90^\circ)$ | $\langle l^2 \rangle$ |
|------------------------|-------------|------------------|---------------------------------------|-----------------------|
| 31.0 | 22.8 | 13.57 ± 0.51 | 3.11 ± 0.06 | 109.796 |
| 32.0 | 23.8 | 16.39 ± 0.56 | 2.94 ± 0.05 | 119.637 |
| 32.5 | 24.3 | 17.69 ± 0.55 | 2.88 ± 0.05 | 124.571 |
| 33.0 | 24.8 | 17.91 ± 0.89 | 2.92 ± 0.08 | 129.512 |
| 33.5 | 25.3 | 21.83 ± 0.66 | 2.68 ± 0.04 | 134.458 |
| 34.0 | 25.8 | 22.97 ± 0.70 | 2.65 ± 0.04 | 139.408 |
| 34.5 | 26.2 | 22.35 ± 0.87 | 2.74 ± 0.06 | 144.362 |
| 35.0 | 26.8 | 24.53 ± 0.86 | 2.66 ± 0.05 | 149.317 |
| 35.5 | 27.2 | 25.63 ± 1.16 | 2.64 ± 0.06 | 154.274 |
| 36.0 | 27.7 | 25.05 ± 0.88 | 2.72 ± 0.05 | 159.232 |
| 36.5 | 28.2 | 28.77 ± 0.97 | 2.56 ± 0.04 | 164.189 |
| 37.0 | 28.7 | 29.59 ± 1.12 | 2.56 ± 0.05 | 169.146 |
| 37.5 | 29.2 | 31.91 ± 1.34 | 2.50 ± 0.05 | 174.103 |
| 38.0 | 29.7 | 34.64 ± 1.36 | 2.43 ± 0.05 | 179.058 |
| 39.0 | 30.7 | 38.88 ± 1.50 | 2.35 ± 0.05 | 188.963 |
| 40.0 | 31.6 | 37.74 ± 1.34 | 2.45 ± 0.04 | 198.859 |
| 41.0 | 32.6 | 37.66 ± 1.25 | 2.52 ± 0.04 | 208.746 |
| 42.0 | 33.6 | 41.28 ± 1.48 | 2.45 ± 0.04 | 218.620 |
| 43.0 | 34.6 | 42.33 ± 1.24 | 2.48 ± 0.04 | 228.483 |
| 44.0 | 35.6 | 44.14 ± 1.46 | 2.48 ± 0.04 | 238.332 |
| 46.0 | 37.5 | 52.43 ± 1.93 | 2.36 ± 0.04 | 257.988 |
| 48.0 | 39.5 | 56.64 ± 2.79 | 2.35 ± 0.06 | 277.586 |
| 50.0 | 41.5 | 60.88 ± 3.04 | 2.34 ± 0.06 | 297.125 |

Berkeley. The mica strips obtained from the experiment were etched with hydrofluoric acid (48%) for 5 to 6 h. In this way the diamond-shaped fission tracks were observed using an optical microscope (Fig. 2) with a total magnification ranging from $60\times$ to $200\times$.

Rectangular strips of the mica were scanned almost

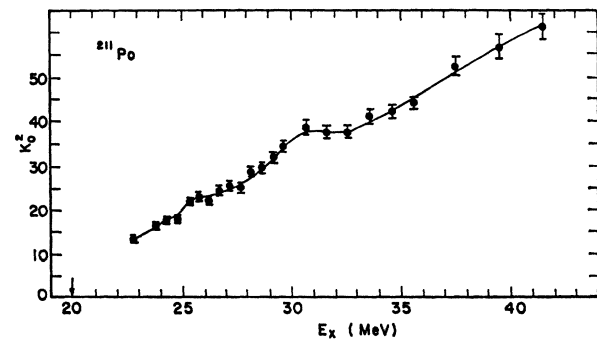


FIG. 8. K_0^2 dependence on excitation energy at the fission saddle point of Po^{211} . The arrow indicates the position of the fission barrier.

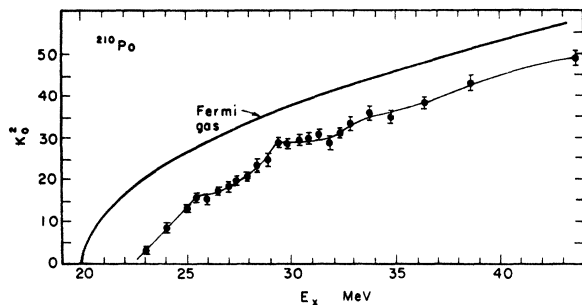


FIG. 9. Experimental values of K_0^2 in Po^{210} compared with the Fermi-gas prediction (see text for the values of the parameters used).

continuously over angles ranging from 85° to 172° . The angular correction for the aberration introduced by the scanning technique is presented in the Appendix. The angular width of the strips was 3° or smaller, since the angular resolution of the system was about 3° .

IV. ANALYSIS OF THE DATA

The experimental angular-distribution data were first transformed to the center-of-mass system. In this case the assumption was made that all of the fission fragments had the same kinetic energy equal to half the average total kinetic energy. The total kinetic energy for ^{210}Po was taken as 146.6 MeV and for ^{211}Po as 146 MeV (see the experimental data of Vandenbosch and Huizenga¹⁸). The dispersion in angle introduced by the variations in kinetic energy of fission fragments and by the neutrons evaporating from the fragments was estimated to be of the order of 1° . The center-of-mass angular distributions were fitted with Eq. (6). The fitting parameters were the value of a normalization constant and the quantity K_0^2 .

The coefficients T_I were obtained from an optical-model calculation on the $^{206}\text{Pb}+^4\text{He}$ and $^{207}\text{Pb}+^4\text{He}$ reactions using a Wood-Saxon potential. The parameters used were

| ^{206}Pb | ^{207}Pb |
|------------------------|------------------------|
| $V = -50$ MeV | $V = -50$ MeV |
| $W = -23.00$ MeV | $W = -23.12$ MeV |
| $r_0 = 1.17A^{1/3}$ fm | $r_0 = 1.17A^{1/3}$ fm |
| $r_\alpha = 1.77$ fm | $r_\alpha = 1.77$ fm |
| $d = 0.576$ fm | $d = 0.576$ fm |

These parameters have been taken or extrapolated from the work of Huizenga and Igo.¹⁹

The effect of the ^{207}Pb target spin $\frac{1}{2}$ on the angular distribution has been neglected. An estimate of such an

¹⁸ R. Vandenbosch and J. R. Huizenga, Phys. Rev. **127**, 212 (1962).

¹⁹ J. R. Huizenga and G. Igo, Nucl. Phys. **29**, 462 (1962).

effect has been done following Griffin.²⁰ The change in the predicted anisotropy has been evaluated and found to be smaller than 1.5%.

Some examples of experimental angular distributions, together with the theoretical fits, are shown in Figs. 3, 4, 5, and 6. The values of K_0^2 versus E obtained from the data fitting are presented in Figs. 7 and 8 and Tables I and II. The quoted errors are calculated from the statistical errors of the experimental data. No other random error has been estimated. The expression for the angular distributions has been found to be very satisfactory in fitting all of the experimental data. The center-of-mass anisotropy $W(180^\circ)/W(90^\circ)$ obtained from the best-fit curves and the average of the square of angular momentum $\langle l^2 \rangle$ obtained from the optical-model calculations are also given in Tables I and II.

V. DISCUSSION

In order to estimate the magnitude of the pairing effects at the saddle point, a knowledge of the fission barriers of the nuclei being considered is essential. The best estimate available at present for the ^{210}Po fission barrier has been obtained by Thompson *et al.*²¹ In their experiments the fission cross sections for the reactions $^{206}\text{Pb}+^4\text{He}$ and $^{209}\text{Bi}+^1\text{H}$ were measured over a large range of energies going down to cross sections as low as 10^{-35} cm². Theoretical expressions derived by Huizenga *et al.*²² and by Burnett *et al.*²³ were used to fit the data expressed in the form of the ratio Γ_f/Γ_n . The fission barriers deduced from fitting the data when the parameters were varied over rather large reasonable ranges averaged 19.82 MeV for $^{209}\text{Bi}+^1\text{H}$ and 20.25 for $^{206}\text{Pb}+^4\text{He}$. These calculations do not include pairing effects. Thus for even-even compound nuclei the level density at the saddle point will tend to make the above values overestimates so that the real barriers should be somewhat lower. Nonetheless, we shall take 20 MeV as the nominal value for ^{210}Po with the mental reservation that the true value could be somewhat lower. This uncertainty means only that the value of the gap estimated in the present work is a lower limit, and the magnitude of the gap could be even larger.

In the case of ^{211}Po , no measured barrier is available. We then rely on two ways of making an estimate: (1) From Myers and Swiatecki's mass formula²⁴ the fission barrier is calculated to be 20 MeV (note that the saddle masses have been normalized to the ^{201}Tl experimental value²³). (2) From Thompson *et al.*²¹ we have taken the measured fission barriers of the following odd nuclei: ^{201}Tl , ^{207}Bi , ^{209}Bi , and ^{213}At and subtracted from them

²⁰ J. J. Griffin, Phys. Rev. **127**, 1248 (1962).

²¹ S. G. Thompson, Arkiv Fysik **36**, 267 (1967).

²² J. R. Huizenga, R. Chaudhry, and R. Vandenbosch, Phys. Rev. **126**, 210 (1962).

²³ D. S. Burnett, R. C. Gatti, F. Plasil, P. B. Price, W. J. Swiatecki, and S. G. Thompson, Phys. Rev. **134**, B952 (1964).

²⁴ W. D. Myers and W. J. Swiatecki, Nucl. Phys. **81**, 1 (1966).

the mass shift due to the shell effect in the ground state. We have plotted these corrected values as a function of the fissility parameter x . By interpolation and correction for the shell effect we obtained for the ^{211}Po barrier about 19.8 MeV, very close to the Myers-Swiatecki predicted value.

Once the barrier height is known, we can make a comparison with the predictions of the Fermi gas model. This model relates K_0^2 to the excitation energy E_s^* over the saddle point as follows²:

$$K_0^2 = (\mathfrak{F}_{\text{eff}}/\hbar^2)T. \quad (7)$$

T is the nuclear temperature at the saddle point which is related to the excitation energy at the saddle point E_s^* by the expression

$$T^2 = E_s^*/a_f, \quad (8)$$

a_f being the level density parameter at the saddle point. The effective moment of inertia $\mathfrak{F}_{\text{eff}}$ is related to the moment of inertia about the symmetry axis \mathfrak{F}_{\parallel} and about an axis perpendicular to it, \mathfrak{F}_{\perp} , by the expression

$$\mathfrak{F}_{\text{eff}}^{-1} = \mathfrak{F}_{\parallel}^{-1} - \mathfrak{F}_{\perp}^{-1}. \quad (9)$$

The values of K_0^2 obtained from both the experimental data and from Eq. (7) are shown in Fig. 9. The value of $\mathfrak{F}_{\text{eff}}$ was taken from the liquid-drop calculations of Cohen and Swiatecki,²⁵ and a_f was taken equal to $A/8$.²⁶ This curve does not represent an actual fitting to the data. It merely indicates the disagreement between theoretical predictions and experimental data. The fact that K_0^2 is lower than predicted on the basis of the Fermi gas assumption can be accounted for in terms of pairing effects. In particular we observe that in the ^{210}Po case, K_0^2 drops rapidly to zero at about 3 MeV above the saddle point. More precisely, at 3 MeV above the "nominal" barrier, $K_0^2 = 3.3$. This value is so small that it can be explained in terms of collective excitation states (rotational and vibrational) within the gap, precluding any substantial contribution by intrinsic (two-quasiparticle) excitations. Also the next higher point has a value $K_0^2 = 8.8$ that could be explained both by collective excitations and intrinsic excitations. This indicates that the pairing gap for ^{210}Po at the saddle point is at least 3 MeV. An immediate check in the ^{211}Po case shows that K_0^2 does not drop to zero even at 3 MeV above the barrier. This is to be expected for an odd nucleus for which a gap is absent because the odd particle provides intrinsic excitations at all energies.

Another large effect that can be observed is the overall difference between the two K_0^2 curves. The ^{211}Po curve follows the trend of the ^{210}Po curve rather well, but lies higher by about 7.5 units of K_0^2 . If this is

an even-odd effect, then we conclude that the average contribution of one neutron quasiparticle to K_0^2 is about 7.5 units. This checks rather well with a calculation based on the Nilsson model. We have calculated the average square of the Ω values of the Nilsson orbitals about the Fermi level. At the maximum deformation available in Nilsson calculations²⁷ ($\epsilon = 0.6$), $\langle \Omega^2 \rangle$ is about 8 for neutrons and 5 for protons (average over 16 levels). With these contributions to K_0^2 of one neutron and proton quasiparticle, one can check whether some of the structure visible in the plots of K_0^2 for ^{210}Po and ^{211}Po is related to the onset of different numbers of quasiparticles. In ^{210}Po two flattenings occur at $K_0^2 \cong 16$ and $K_0^2 \cong 29$, values which are consistent with two- and four-quasiparticle configurations, respectively. In ^{211}Po two flattenings occur at $K_0^2 \cong 22.5$ and $K_0^2 \cong 37.5$ values, again very close to the expected ones for three- and five-quasiparticle configurations. The very definite possibility of different values for the gap parameter for neutrons and protons makes it difficult to decide the quantitative significance of the above structure. However, their positions in excitation energy, as well as the absolute values of K_0^2 as a function of energy, when compared with the one-quasiparticle contributions, still suggest a rather larger value for the pairing gap than the lower limit previously discussed, possibly 4 MeV or larger.

A. Gap Parameter from Even-Odd Mass Differences at the Saddle Point

The difference in fission barriers between odd- A and even-even isotopes can provide in principle some information about the gap parameter Δ_s at the saddle point, just as the ground-state even-odd mass differences allow the evaluation of the ground-state gap parameter Δ_g . It is therefore of interest to analyze this problem since we have reasonably good values for the fission barriers of ^{210}Po and ^{211}Po .

Let us assume with Myers and Swiatecki²⁴ and Strutinski²⁸ that shell and pairing effects are separable from a smooth liquid-drop-like term. This term can be derived from a pure single-particle model with smoothly varying level spacing and including surface, symmetry, Coulomb energy, and any other term which is of single-particle and electromagnetic nature. Using such a single-particle model for the energy base line, we can express the fission barrier of an even-even nucleus $B_{f,e}$ as follows (see Fig. 10):

$$B_{f,e} = B_{\text{sp},e} + \text{Shell}_{g,e} + C_{g,e} - \text{Shell}_{s,e} - C_{s,e}, \quad (10)$$

where $B_{\text{sp},e}$ is the term deriving from the single-particle (liquid-drop-like) model.

²⁵ S. Cohen and W. J. Swiatecki, Ann. Phys. (N.Y.) **22**, 406 (1963).

²⁶ K. J. LeCouteur and D. W. Land, Nucl. Phys. **13**, 32 (1959).

²⁷ C. Gustafson, I. L. Lamm, B. Nilsson, and S. G. Nilsson, Arkiv Fysik **36**, 613 (1967).

²⁸ V. M. Strutinski, Arkiv Fysik **36**, 629 (1967).

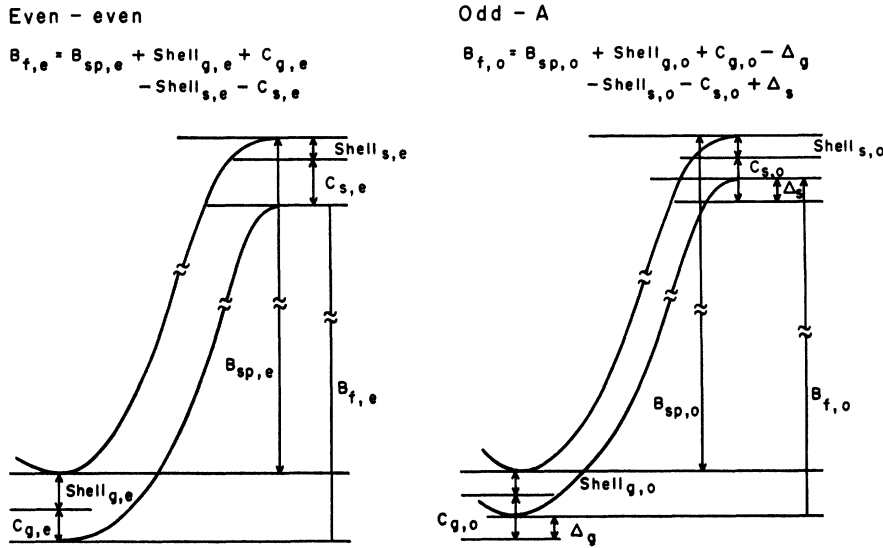


FIG. 10. Schematic representation of the fission barrier of an even-even and odd- A nucleus in terms of a smooth single-particle model plus shell and pairing effects.

$Shell_{g,e}$ and $Shell_{s,e}$ are the shell terms in the ground state and saddle point, respectively, due to the bunching of single-particle levels.

$C_{g,e}$ and $C_{s,e}$ are the condensation energies due to pairing in the ground state and saddle point, respectively.

In order to obtain the fission barrier for an odd- A nucleus, we must add the lowest one-quasiparticle excitation to both the paired ground state and saddle point of the corresponding even-even nucleus; we can also make allowance for smooth changes due to the introduction of the extra particle. The one-quasiparticle excitation energy is

$$E = [(\epsilon - \lambda)^2 + \Delta^2]^{1/2} \approx \Delta,$$

where λ is the Fermi level and ϵ is the energy of the single-particle level closest to it. Then the fission barrier $B_{f,o}$ for an odd- A nucleus can be written as follows (see Fig. 10):

$$B_{f,o} = B_{sp,o} + Shell_{g,o} + C_{g,o} - \Delta_g - Shell_{s,o} - C_{s,o} + \Delta_s, \quad (11)$$

where Δ_g and Δ_s are the gap parameters at the ground and saddle point, respectively, and the other terms are the equivalent to those described in the previous expression.

From (10) and (11) we obtain

$$\begin{aligned} \Delta_s - \Delta_g = & (B_{f,o} - B_{f,e}) - (B_{sp,o} - B_{sp,e}) \\ & - (Shell_{g,o} - Shell_{g,e}) + (Shell_{s,o} - Shell_{s,e}) \\ & - (C_{g,o} - C_{g,e}) + (C_{s,o} - C_{s,e}). \quad (12) \end{aligned}$$

The two terms $(C_{g,o} - C_{g,e})$ and $(C_{s,o} - C_{s,e})$ should be small because the main effect of the odd particle is included in the one-quasiparticle excitation and should be of negative sign because of the blocking effect of the odd particle. Since the two terms appear with opposite sign, one might disregard them for lack of better knowledge.

The term $(Shell_{s,o} - Shell_{s,e})$ is likely to be small for large saddle deformations. The term $(Shell_{g,o} - Shell_{g,e})$ is dependent on the position of the two nuclei with respect to a closed shell and can be as large as a few MeV; therefore, it cannot be disregarded.

The term $(B_{sp,o} - B_{sp,e})$ can be evaluated from liquid-drop calculations, and its magnitude is of the order of a few tenths of 1 MeV if the odd particle is a neutron and of the order of 1 MeV if the odd particle is a proton.

The relation

$$\Delta_s - \Delta_g = B_{f,o} - B_{f,e} \quad (13)$$

has been used by Stepien and Szymanski.²⁹ It seems from the above considerations that such an expression could be very unreliable in obtaining the saddle-point gap parameter Δ_s .

We can now apply Eq. 12 to the ^{210}Po , ^{211}Po pair to estimate the gap parameter Δ_s at the saddle point. If we take the fission barrier values previously discussed and the shell effects and liquid-drop terms from Myers and Swiatecki,²⁴ we obtain $\Delta_s - \Delta_g = 1.0$ MeV; it is difficult to establish the uncertainties of this quantity, but, on the basis of the discussion of the ^{210}Po fission barrier in Sec. IV, it could be somewhat larger. Using for Δ_g the value of 0.81 MeV given by Nemirovsky and Adamchuk³⁰ (this value, obtained from even-odd mass differences, has been corrected for shell effects and other liquid-drop contributions), we obtain $\Delta_s = 1.81$ MeV and then the pairing gap $2\Delta_s = 3.62$ MeV, in agreement with the value obtained from the angular distribution analysis.

B. Possible Reasons for the Large Pairing Effects

There is no satisfactory explanation as yet for the very large pairing effects observed at the saddle point.

²⁹ W. Stepien and Z. Szymanski, Phys. Letters **26B**, 181 (1968).

³⁰ P. E. Nemirovsky and Yu. V. Adamchuk, Nucl. Phys. **39**, 551 (1962).

However, it is interesting to consider some possible causes of such effects.

From the uniform model, the gap parameter Δ can be expressed approximately in terms of the density g of Nilsson levels near the Fermi level and pairing strength G as follows:

$$\Delta = S e^{-1/gG}, \quad (14)$$

where S is the energy interval above and below the Fermi surface over which the pairing interaction extends.

An accidental bunching of levels about the Fermi surface at the saddle-point deformation could in principle result in an increase in g sufficient to explain the observed effect. However, such an explanation may be ruled out if the experimental results continue to show more cases in which a larger value of Δ is observed at the saddle point than in the ground state, especially if the observations are made over a large range of deformation. Even the present data together with the data available for ^{236}U and ^{240}Pu tend to rule out the hypothesis that the effect is due only to the accidental bunching of levels. An increase of pairing strength G with an increase in the surface of the nucleus resulting from deformation is considered to be a more likely explanation.

The dependence of the gap parameter Δ on the nuclear surface has been studied by Kennedy *et al.*¹³ They observed that infinite-nuclear-matter calculations with realistic nucleon-nucleon potentials yielded very low values for the pairing gap. The physical reason for this effect can be understood as follows: The Fermi momentum for the nuclear-matter density corresponds to collision energies of about 80 MeV in the center-of-mass between two nucleons. At this energy the repulsive core in the nucleon-nucleon potential approximately compensates for the attractive part of the potential. On the other hand, a calculation carried out for a slab of nuclear matter of finite thickness and infinite extension yielded a substantial pairing gap whose magnitude was very sensitive to the slab thickness. This can be understood by noting the lower density in the surface region. The lower density implies a lower Fermi momentum, for which the hard core of the nucleon-nucleon potential is not strongly felt.

Stepien and Szymanski²⁰ attempted to explain the large pairing gap at the saddle point by assuming that the pairing strength increases proportionally to the nuclear surface as the nucleus deforms from the equilibrium configuration to the saddle point. They also quote some results of gap-parameter calculations carried on in the rare-earths region. In these calculations the BCS equations were solved for increasing values of the pairing strength. By making the same assumptions we can obtain a general approximate relation between Δ and s .

We write

$$G = G_0 [1 + (\delta s/s)], \quad (15)$$

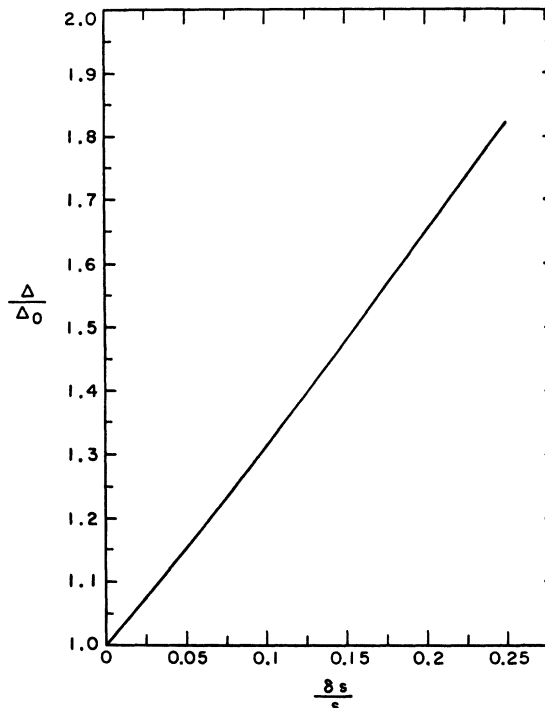


FIG. 11. Dependence of the gap parameter on the nuclear surface calculated using the assumption of Stepien and Szymanski.

where $\delta s/s$ is the fractional surface increase; substituting in (14), we obtain

$$\ln \frac{\Delta}{\Delta_0} = \frac{1}{gG_0} \left[\frac{\delta s/s}{1 + (\delta s/s)} \right]. \quad (16)$$

The quantity gG_0 is dimensionless and has a value of about $\frac{1}{3}$. The increase in Δ as a function of $\delta s/s$ is presented in Fig. 11. The agreement between this general calculation and the specific case reported by Stepien and Szymanski is good, but it appears that the increase in gap predicted in this way is not quite large enough to reproduce the experimental data.

ACKNOWLEDGMENTS

We would like to thank J. R. Nix, W. J. Swiatecki, and S. G. Nilsson for their helpful discussions and suggestions. We are indebted to N. Glendenning for the use of his optical-model program. We are very grateful to Mrs. Claudette Ruge for the development of the program to fit the angular-distribution data.

APPENDIX: ANGULAR CORRECTION

The fission fragments coming at a given angle θ with respect to the beam axis constitute a cone which intercepts the cylindrical surface on which mica is present. When the mica is flattened out on a plane the equation of intercept in cylindrical coordinates will be (see

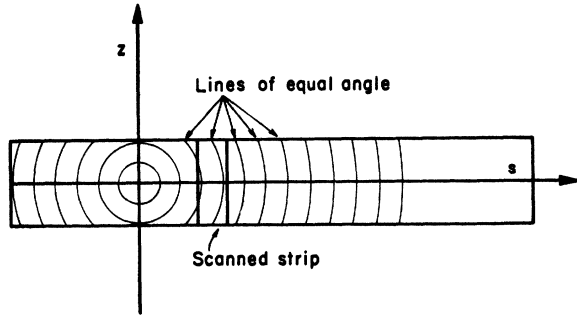


FIG. 12. Drawing of a mica strip with lines of equal angle. The scanning is carried on in rectangular strips as indicated in the figure.

Fig. 12)

$$z^2 = R^2 \left(\frac{\cos^2(S/R)}{\cos^2\theta} - 1 \right), \quad (17)$$

where $R = \rho$ and $S/R = \omega$.

When the mica scan is done in rectangular strips as shown in Fig. 12, one has to introduce a correction in the measured angular distribution due to the angular aberration. If the true angular distribution can be considered linear within the maximum and minimum θ values in the strip, the correction can be done exactly by substituting the nominal angle with the weighted average of the angle within the strip

$$\bar{\theta} = \left(\int_{-z_{\max}}^{+z_{\max}} \int_{S_1}^{S_2} \theta(S, z) dS dz / 2z_{\max}(S_2 - S_1) \right). \quad (18)$$

The quantity $\theta(S, z)$ can be obtained from Eq. (17):

$$\theta(S, z) = \cos^{-1} \frac{\cos(S/R)}{[1 + (z^2/R^2)]^{1/2}}. \quad (19)$$

The double integral can then be evaluated numerically or the following approximation can be used:

$$\begin{aligned} z^2/R^2 &\ll 1, \\ \theta(S, z) &= \cos^{-1} \left[\left(1 - \frac{1}{2} \frac{z^2}{R^2} \right) \cos \frac{S}{R} \right] \\ &= \cos^{-1} \left[\cos \left(\frac{S}{R} + \delta \right) \right]. \quad (20) \end{aligned}$$

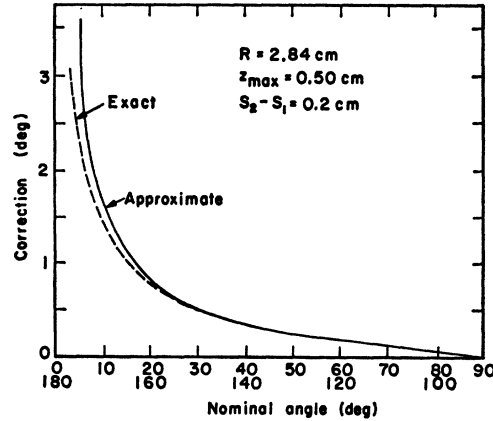


FIG. 13. Correction for the angular aberration introduced by the scanning technique. The two curves correspond to the exact and approximate expressions given in the text.

Expanding $\cos[(S/R) + \delta]$ to first order in δ and equalizing the expression to $[1 - \frac{1}{2}(z^2/R^2)] \cos(S/R)$, one obtains

$$\delta = \frac{1}{2} (z^2/R^2) [\tan(S/R)]^{-1}. \quad (21)$$

Then Eq. (19) becomes

$$\theta(S, z) = (S/R) + \frac{1}{2} (z^2/R^2) [\tan(S/R)]^{-1}. \quad (22)$$

With this approximate form, the double integral (18) can be evaluated in closed form and the result is

$$\bar{\theta} = \frac{S_2 + S_1}{2R} + \frac{1}{6} \frac{z_{\max}^2}{R(S_2 - S_1)} \ln \frac{\sin(S_2/R)}{\sin(S_1/R)} \quad (23)$$

or

$$\bar{\theta} = \theta_{\text{nom}} + \frac{1}{6} \frac{z_{\max}^2}{R(S_2 - S_1)} \ln \frac{\sin(S_2/R)}{\sin(S_1/R)}. \quad (24)$$

Since the expression (21) does not behave well near 0° , expression (24) cannot be used for very small angles, which in general are not accessible anyway. A comparison between the exact and the approximate expression is shown in Fig. 13.

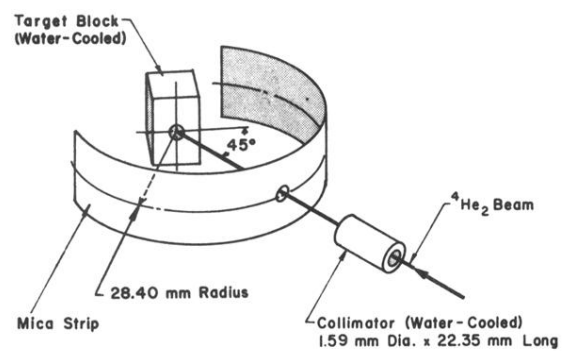


FIG. 1. Schematic drawing of the apparatus used in measuring angular distributions of fission fragments.

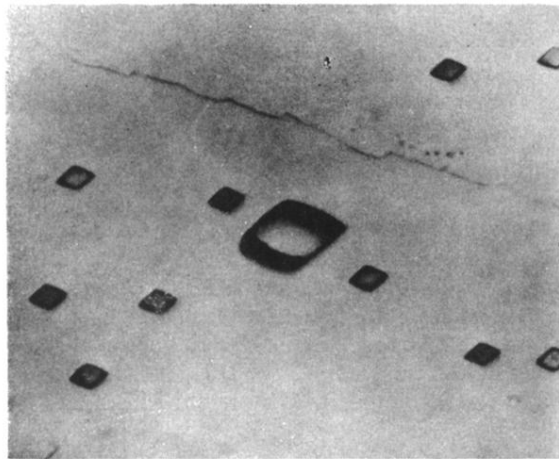


FIG. 2. Fission tracks in mica. Etching: 6 h at room temperature in 48% hydrofluoric acid. The fission fragments have entered perpendicularly to the mica surface; therefore the picture shows the normal sections of the tracks. The large track is a pre-etched background track due to spontaneous fission of U^{238} in mica.